Crashworthiness of Composite Structures with Various Fiber Architectures

Nageswara R. Janapala[1], Fu-Kuo Chang[2], Robert K. Goldberg[3],
Gary D. Roberts[4] and Karen E. Jackson[5]
[1]*Dept. of Mechanical Engineering, Stanford University, Stanford, CA*
[2]*Dept. of Aeronautics and Astronautics, Stanford University, Stanford, CA*
[3]*Mechanics and Life Prediction Branch, NASA Glenn Research Center, Cleveland, OH*
[4]*Materials and Structures Branch, NASA Glenn Research Center, Cleveland, OH*
[5]*Structural Dynamics Branch, NASA Langley Research Center, Hampton, VA*
jnrao@stanford.edu; fkchang@stanford.edu; robert.goldberg@nasa.gov;
gary.d.roberts@nasa.gov; Karen.E.Jackson-1@nasa.gov

Abstract

Advanced textile composite structures, such as braids and fabrics, are showing promising characteristics for energy absorption. However, modeling of these composite structures is quite challenging because of their complicated architecture, varied fiber/matrix combinations, and the failure mechanisms associated with them. Unfortunately, none of the existing material models is capable of simulating diverse failure behaviors observed during crushing of these composite structures. This paper will present a material model that can simulate the crushing response of composite structures with different fiber architectures. The material model identifies a smallest repeatable unit (i.e. unit-cell) within the textile composite and considers fiber modeling, strain rate effect, tow rotation and progressive failure criteria at tow level. The composite tow is assumed to be transverly isotropic, and modeled using an elastic-viscoplastic constitutive law. A DyCrash (Dynamic Crash) module is developed and implemented in LS-DYNA® as a user routine. The module is currently being validated for Kevlar fabrics. Results are presented for $0^0/90^0$ and $\pm 45^0$ Kevlar fabric coupons. A methodology is developed to back calculate the yarn properties from available Kevlar fabric test data using DyCrash.

Introduction

Crashworthiness, the ability of a structure to protect its occupants during crash, is still a major challenge in the design of next generation structures in the aerospace, automobile, mechanical and allied areas. Next generation structures must be designed based on several aspects including for example light weight for fuel efficiency, stiffness and strength for dynamic performance, impact damage tolerance and crashworthiness design for safety. Composite structures have been replacing current metallic structures because of their excellent specific strength, stiffness and energy absorption [1]. The finite element methods (FEM) based on the continuum mechanics of plasticity have been extensively applied to crash simulation of metallic structures with the help of commercially available codes such as LS-DYNA. Unfortunately, the experience accumulated from modeling of metallic structures is hardly transferable to composite structures under crushing loads because the failure mechanisms and the deformation modes in composites are much more complicated compared with metallic structures. Many attempts to simulate the crashworthiness of composite structures using continuum damage models have resulted in either too many non-measurable parameters or inaccurate predictions [2-3].

Textile composites are known to have better out-of-plane strength and specific stiffness as compared to the tape-laminated composites [4]. These composites can be manufactured with a high level of automation and can also be produced as net-shape parts, both of which are

advantageous for several industries. However, the complex fabric architecture makes analysis of these composites difficult. Various models, starting from simple analytical models to complex numerical models, exist in the literature to analyze these fabrics. Linear elastic models are used to predict stiffness and strength properties [4-5]. A survey of various modeling approaches to model the fabrics is given by Cox and Flanagan [6]. Analytical methods make use of general continuum mechanics equations and laws, such as the conservation of energy and momentum. These methods are useful to handle simple physical phenomena, but become increasingly complicated as the phenomena become more complex. In unit-cell based methods [7-9], the fabric geometry is usually represented by a unit-cell, which by repeated translation will yield the entire fabric structure. This unit-cell is then divided into segments and a homogenization scheme is applied to calculate strains, and stresses. Various researchers [7-9] explored this approach to calculate the stiffness and the stress-strain behavior of the fabrics. In general, this approach reduces the computational effort required to model the complex structures.

Unfortunately, there is no single material model available in the literature that can simulate the various failure modes observed during the crushing of textile composites with various fabric/matrix combinations. This paper presents the DyCrash module, that is developed in-house and linked with commercially available FE package LS-DYNA, to simulate the crushing response of various textile architectures by choosing the different fiber/matrix combinations. The material model employed in our DyCrash module identifies a smallest repeatable unit (i.e. unit-cell) within the textile composite and considers different fiber behaviors, strain rate effect, tow rotation and progressive failure criteria at the tow level. The composite tow is assumed to be transversely isotropic and modeled using an elastic-viscoplastic constitutive law. Stiffening and straightening behavior of the unit-cell is considered at the tow level. The following section briefly discusses various models that are implemented in the DyCrash module. Complete details of these material models are available in Beard and Chang [10] and Flesher [11].

DyCrash module

The DyCrash module is based on a unit-cell model for different textile architectures. It incorporates an elastic-viscoplastic constitutive model including rate effects, stiffening and scissoring mechanism, and progressive failure criteria. The DyCrash module is extensively validated for Carbon/epoxy tri-axial braided system [11].

Unit-cell model

Flesher [11] derived a simplified unit-cell model for 2D tri-axial braided composites. A similar unit-cell model for plain weave fabrics is derived by Janapala and Chang [12]. Figure 1 shows typical unit-cells of tri-axial braid and plain weave fabrics. The unit-cell consists of impregnated warp and fill (weft) yarns, which are orthogonal to each other. The yarns are described by prismatic segments within the unit-cell. Undulation in both the warp and fill yarns is considered. Each yarn segment is described by the in-plane angle (θ) and out-of-plane angle (β). The in-plane angle is the angle made by the tow segment with the X-axis and the out-of-plane angle is the angle made by the tow segment with the X-Y plane. For plain weave architectures, θ will be either 0 (warp) yarns or 90 (fill) yarns. The β represents the undulation in the yarn, which is calculated based on the architecture of the fabric. Volume fractions for different segments are

calculated based on the unit-cell model and these fractions are used in calculating the homogenized properties.

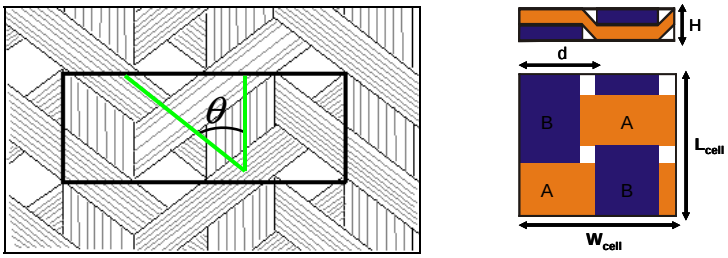

Figure 1: Typical unit-cells of tri-axial braids and plain weave fabrics

Elastic and visco-plastic model

Tows are made of bundles of fibers held together with the matrix material. Figure 2 shows the tow segment in its local coordinate system. Transversely isotropic behavior is assumed for each tow segment within the unit-cell.

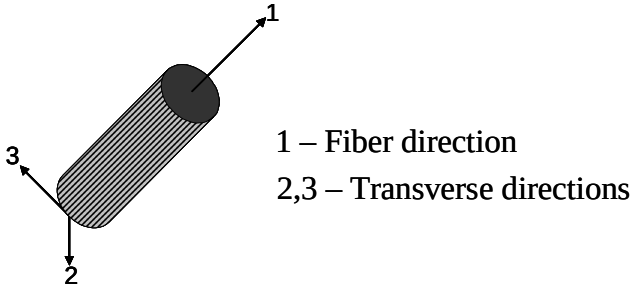

Figure 2: Tow segment within the unit-cell

Flesher [11] implemented a visco-plastic material model to simulate the dynamic behavior of carbon/epoxy braided composites based on isotropic hardening. This rate-dependent material model is based on the extension of the 2D visco plasticity model of Sun and co-workers [13-14]. Isotropic hardening, widely used in large dynamic problems, assumes that the center of the yield surface remains stationary in stress-space but the radius expands due to strain hardening. A general quadratic form of a plastic potential function is assumed that satisfies orthotropic symmetry [15] and is represented as:

$$2f = a_{11}\sigma_{11}^2 + a_{22}\sigma_{22}^2 + a_{33}\sigma_{33}^2 + 2a_{12}\sigma_{11}\sigma_{22} + 2a_{13}\sigma_{11}\sigma_{33} + 2a_{23}\sigma_{22}\sigma_{33} + 2a_{44}\sigma_{23}^2 + 2a_{55}\sigma_{13}^2 + 2a_{66}\sigma_{12}^2$$

Flesher [11] assumed that all the plasticity in the carbon/epoxy braided composite tows arises from the matrix material, the fibers behave in a linear-elastic manner and uniform dilation does not influence plastic deformation. The general quadratic equation is thus reduced to:

$$2f(\sigma_{ij}) = (\sigma_{22} - \sigma_{33})^2 + 4\sigma_{23}^2 + 2a_{66}(\sigma_{12}^2 + \sigma_{13}^2)$$

Carbon fibers are very brittle but Kevlar fibers are ductile particularly in compression. Figures 3 and 4 show the schematic representation of Carbon and Kevlar fibers behavior observed in the experiments. Due to the ductile nature, Kevlar fibers suffer from having very low compression strength as compared to the Carbon fibers. The linear elastic assumption in the fiber direction is erroneous to represent the behavior of Kevlar fibers in compression. Hence for the Kevlar tows,

we have assumed that plasticity comes from both the fiber and the matrix material. A general quadratic function for orthotropic materials will be used for the Kevlar tows.

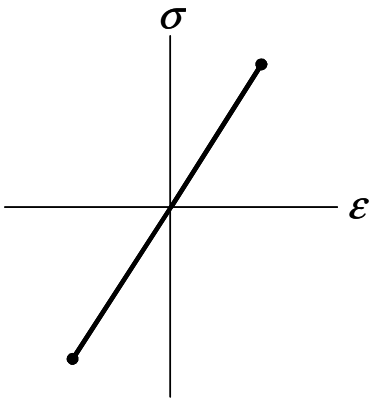

Figure 3: Carbon fiber

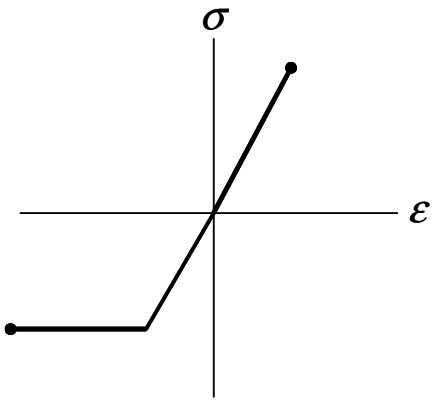

Figure 4: Kevlar fiber

The associative-flow rule is expressed as [14]: $d\varepsilon_{ij}^{p} = d\lambda \dfrac{\partial f}{\partial \sigma_{ij}}$

A power-law plasticity model based on Weeks and Sun [14], starting with the effective stress and the plastic work increment.

$$\bar{\sigma} = \sqrt{3 f}$$

$$dW^{p} = \sigma_{ij} d\varepsilon_{ij}^{p} = \bar{\sigma} d\bar{\varepsilon}^{p}$$

This relationship can then be fitted with a power-law: $\bar{\varepsilon}^{p} = A(\bar{\sigma})^{n} = \chi(\dot{\bar{\varepsilon}}^{p})^{m}(\bar{\sigma})^{n}$

The visco-plastic compliance matrix is fully populated for Kevlar tows and is given as:

$$S^{VP} = \begin{bmatrix} S_{11}^{VP} & S_{12}^{VP} & S_{13}^{VP} & S_{14}^{VP} & S_{15}^{VP} & S_{16}^{VP} \\ S_{12}^{VP} & S_{22}^{VP} & S_{22}^{VP} & S_{24}^{VP} & S_{25}^{VP} & S_{26}^{VP} \\ S_{13}^{VP} & S_{22}^{VP} & S_{22}^{VP} & S_{24}^{VP} & S_{25}^{VP} & S_{26}^{VP} \\ S_{14}^{VP} & S_{24}^{VP} & S_{24}^{VP} & S_{44}^{VP} & S_{45}^{VP} & S_{46}^{VP} \\ S_{15}^{VP} & S_{25}^{VP} & S_{25}^{VP} & S_{45}^{VP} & S_{55}^{VP} & S_{56}^{VP} \\ S_{16}^{VP} & S_{26}^{VP} & S_{26}^{VP} & S_{46}^{VP} & S_{56}^{VP} & S_{66}^{VP} \end{bmatrix}$$

The power law mentioned above contains 4 parameters: χ, m, n, and a_{66}, contained within the effective stress. Parameter A is for use at quasi-static rate which includes in itself both χ and m. The parameters above are also strain-rate independent, leaving the rate dependence in the function solely to the effective plastic strain rate term.

A homogenization scheme [11] is used to calculate the average properties of the unit-cell based on the uniform global strain assumption:

$$[C]_{eff} = \sum_{m=1}^{N} v_m [T]_m^T [C] [T]_m$$

where, $[C]$ includes both elastic and visco-plastic stiffness matrices and v_m is the volume fraction of each tow segment.

Scissoring model

Textile composites exhibit a very interesting phenomenon called scissoring during biased loading [10]. When there are gaps between tows or the matrix material is damaged, then the tows rotate until they are jammed (i.e. the condition when the tows touch each other) against each other. The scissoring mechanism affects the overall constitutive behavior of the unit-cell. During scissoring the braid/fabric becomes more compliant and the stiffness increases considerably when the jamming occurs. Beard and Chang [10] derived a scissoring model for braided composites, which is equally applicable for Kevlar fabrics. An idealized stress-strain diagram to account for scissoring (for example, in the Y-direction) is shown in Figure 5. Figure 6 shows the change in braid angle during scissoring.

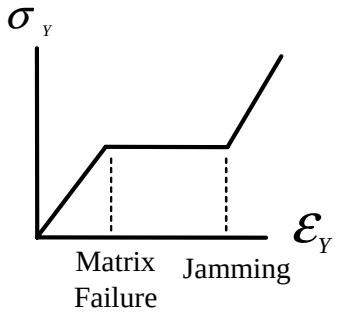

Figure 5: Idealized stress-strain diagram during scissoring

When the unit-cell is undeformed, the fabric angle is given as

$$\theta^o = \tan^{-1}\left(\frac{L_Y}{L_X}\right)$$

The updated braid/fabric angle before scissoring is given as

$$\theta^{NEW} = \tan^{-1}\left(\frac{L_Y(1+\varepsilon_{YY})}{L_X(1+\varepsilon_{XX})}\right)$$

The updated braid/fabric angle during scissoring is given as

$$\theta^{NEW} = \sin^{-1}\left(\frac{1+\varepsilon_{YY}}{1+\varepsilon_{YY}^{mf}}\right)$$

where, ε_{XX}, ε_{YY}, ε_{YY}^{mf} are the global strains of the unit-cell in the x, y directions, at matrix failure respectively.

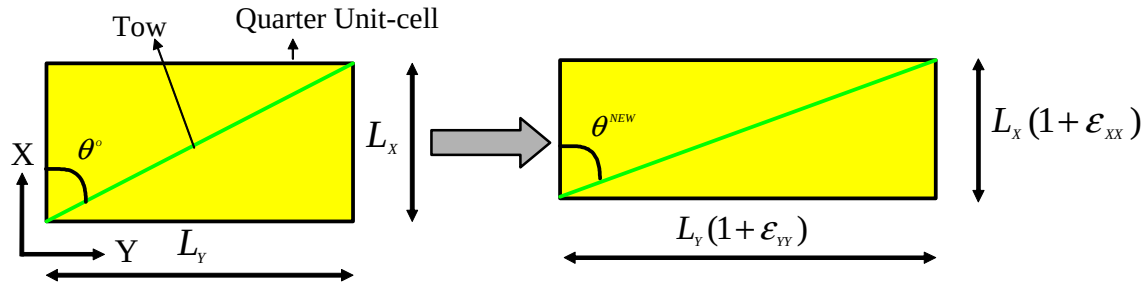

Figure 6: Updated braid angle during scissoring

Stiffening model

It has been observed from the experiments that the average response of the 0/90 Kevlar fabrics exhibited slight stiffening at higher loads. Figure 7 shows the cross-section of the unit-cell before and after application of the load. The undulated portion of the fabric tries to straighten after the matrix failure. Due to this straightening mechanism, the stiffness of the fabric in the direction of the load increases. Figure 8 shows the cross-sectional view of the unit-cell model. The out-of-plane angle (β) change is the measure of the stiffness increase. The updated out-of-plane angle (β) is given as:

$$\beta^{NEW} = \tan^{-1}\left(\frac{H(1+\varepsilon_{zz})}{(d-w)(1+\varepsilon_{YY})}\right)$$

where, *d*, *w*, *H* are the tow spacing, width and unit-cell thickness respectively.

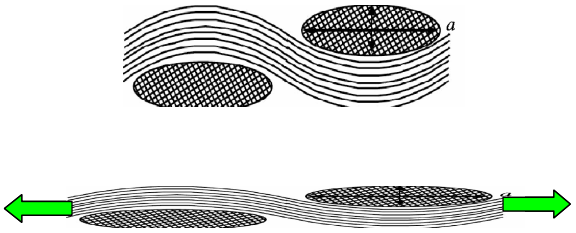

Figure 7: Cross-sectional view of fabric

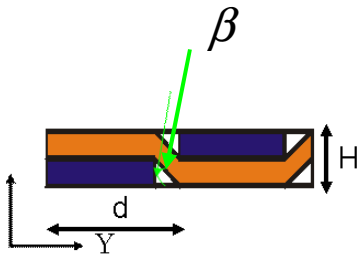

Figure 8: Cross-section of unit-cell

Progressive failure model

The maximum stress failure criteria are applied independently to the tow segments and resin pockets [11]. Table 1 lists the failure criteria and the associated degradation as implemented in the "DyCrash".

Failure	**Critera**	**Degraded Properties**
Tow Tension	$\sigma_{11} \geq X_T$	$E_1 = 0\ G_{12} = 0\ G_{13} = 0$
Longitudinal Tow Compression	$\sigma_{11} \leq X_C$	$\sigma_1 = X_C, \Delta\sigma_1 = 0$ (perfectly plastic)
Transverse Tow Tension	$\sigma_{22} \geq Y_T$	$E_2 = 0,\ G_{12} = 0,\ G_{23} = 0$
	$\sigma_{33} \geq Y_T$	$E_3 = 0, G_{13} = 0,\ G_{23} = 0$
Transverse Tow Compression	$\sigma_{22} \leq Y_C$	$\sigma_2 = Y_C,\ \Delta\sigma_2 = 0$ (perfectly plastic)
	$\sigma_{33} \leq Y_C$	$\sigma_3 = Y_C, \Delta\sigma_3 = 0$ (perfectly plastic)
Shear	$\lvert\sigma_{12}\rvert \geq SS_{12}$	$G_{12} = 0$
	$\lvert\sigma_{13}\rvert \geq SS_{13}$	$G_{13} = 0$
	$\lvert\sigma_{23}\rvert \geq SS_{23}$	$G_{23} = 0$
Matrix pocket failure	$\sigma_I \geq X_{MT}$	$E_M = 0\ G_M = 0$

Table 1: Failure Criteria

Implementation of DyCrash in LS-DYNA

The DyCrash module is implemented in umat41 for shell elements and in umat43 for solid elements. The strain in the out-of-plane normal direction is calculated for shell elements based on a zero normal stress assumption. Quasi-static simulations are performed by scaling up the density artificially such that the kinetic energy is less than 10 percent of total energy.

Input to DyCrash

The DyCrash module requires unit-cell parameters, tow and matrix properties and visco-plastic parameters as an input. The elastic and visco-plastic constants for a given material system are characterized by conducting coupon tests. The detailed procedure to characterize the material constants is described by Flesher [11]. Figure 9 shows the actual and simplified model of the Kevlar plain weave fabric unit-cell. Tables 2-5 list all the inputs that are required by the DyCrash module. As per manufacturer's specification, Kevlar-129 with weave style 726 yarns consists of 600 filaments. Each filament is 12 microns in diameter. Table 2 lists the unit-cell parameters measured from a sample piece of Kevalr-129 fabric under microscope. A total volume fraction of 60 percent is assumed. Other unit-cell parameters such as volume fractions of each segment and the out-of-plane crimp angle are calculated by DyCrash.

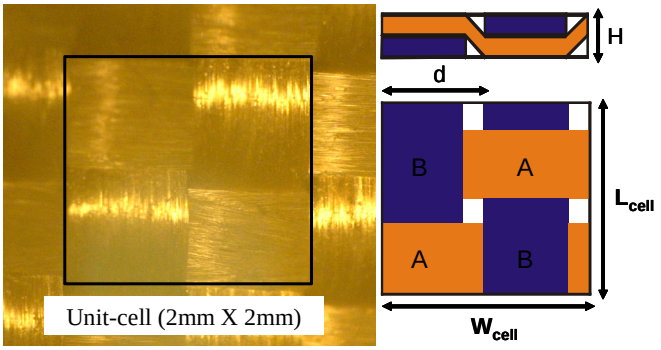

Figure 9: Kevlar fabric unit-cell

Parameter	Value [mm]
H	0.25
d	1.0
L_{cell}	2.0
W_{cell}	2.0

Table 2: Measured unit-cell parameters

E_1 (GPa)	E_2 (GPa)	E_3 (GPa)	G_{12} (GPa)	G_{13} (GPa)	G_{23} (GPa)	ν_{12}	ν_{13}	ν_{23}	E_m (GPa)	G_m (GPa)	ν_m
15	3.5	3.5	2.2	2.2	2.2	0.36	0.3	0.3	3.5	1.3	0.3

Table 3: Kevlar tow and matrix stiffness properties

X_t	X_c	Y_t	Y_c	S	X_m	Y_m	S_m
1500	-100	100	-200	20	35	35	50

Table 4: Kevlar tow and matrix strength properties [MPa]

a_{11}	a_{22}	a_{33}	a_{23}	a_{44}	a_{55}	a_{66}	XN	A
1.0	1.0	1.0	-1.0	2.0	5.5	5.5	5.42	2.95

Table 5: Visco-plastic parameters

Results

Coupon-level tests were performed on Kevlar-129 fabric/epoxy specimens with weave style 726 in $0^0/90^0$ and ± 45^0 orientations [16]. The specimens were fabricated using a Ren Infusion 8601 epoxy purchased from Huntsman with a Ren Activator 8602. The $0^0/90^0$ tests were conducted at 1 ipm (inch per minute) and the $\pm 45^0$ tests were performed at 20 ipm.

A coupon FE model is developed in LS-PrePost® with the same dimensions, 100 mm X 25 mm X 0.3048 mm, as in the tests. Figure 10 shows the coupon model that is meshed with 3D brick elements (*SECTION_SOLID with ELEFORM=2) available in LS-DYNA. A rigid body (*MAT_RIGID keyword is used as material model) is created and tied to top side of coupon by using the *CONTACT_TIED_SURFACE_TO_SURFACE_OFFSET option. Bottom side of the coupon model is given fixed boundary conditions by using *BOUNDARY_SPC_SET keyword. Velocity boundary conditions are applied to the rigid body by using keyword *BOUNDARY_PRESCRIBED_MOTION_RIGID. Several numerical Design of Experiments (DoEs) are performed to back calculate the unidirectional Kevlar 129 yarn properties from the test data on the Kevlar fabrics.

$0^0/90^0$ fabric tension

The simulations started by assuming the tow properties in the transverse direction same as those of matrix elastic properties. Table 7 lists the assumed Kevlar tow and matrix properties and Table 8 lists the visco-plastic parameters used in all the simulations. A volume fraction of 60 percent is assumed. Tables 3-4 list the initially assumed stiffness and strength properties and Table 5 lists the assumed visco-plastic parameters used in the simulation.

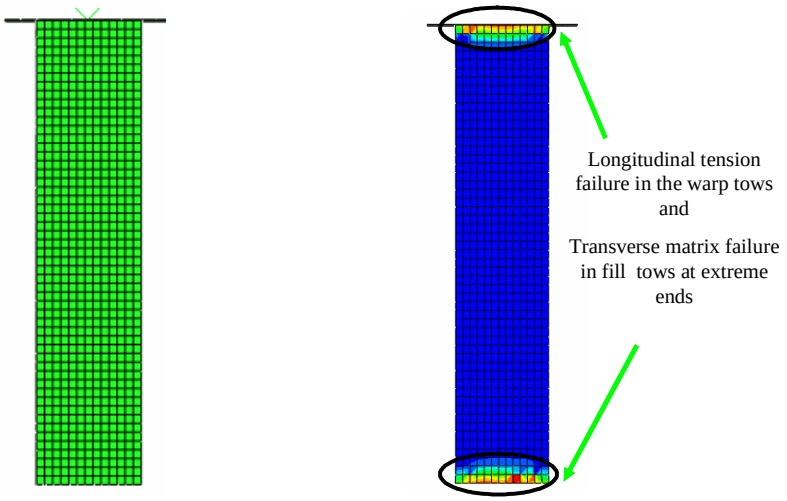

Figure 10: Meshed model and the failure regions of $0^0/90^0$ coupon in tension

Figure 11 compares the computed results to the average stress-strain response of $0^0/90^0$ Kevlar coupons obtained experimentally. Fairly linear behavior with slight stiffening at higher loads is observed in the $0^0/90^0$ coupons. The tow properties in the fiber direction are calculated by tuning the average stress-strain response of $0^0/90^0$ coupons in the simulations with the experimental results. It can be seen that the response predicted by including stiffening effects as well as the failure criteria are matching well with the experimental data. The final failure modes

of the coupon as predicted by the DyCrash are shown in Figure 10. The failure is initiated by transverse matrix cracking in the fill tows and the final failure is due to the longitudinal failure of warp tows. The best estimate of the tow bundle Young's modulus in the fiber direction is approximately 21 GPa. The tensile strength of the tow in the fiber direction and transverse direction are estimated as 1.6 GPa and 0.3, GPa respectively.

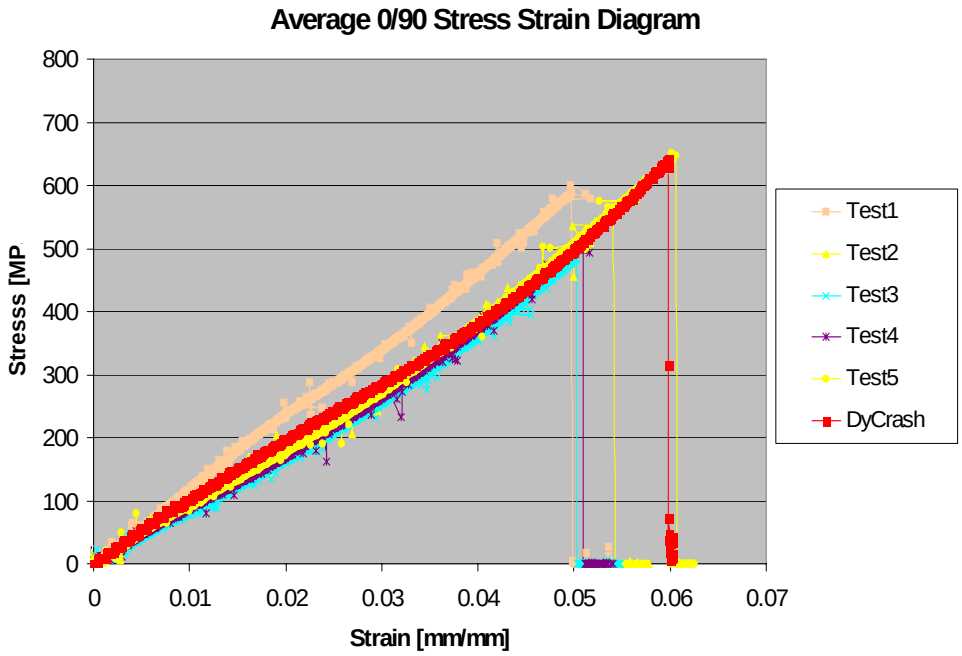

Figure 11: Comparison of average stress-strain response of Kevlar $0^0/90^0$ coupon

± 45^0 fabric tension

The scissoring model is activated in the DyCrash module during the ±45^0 coupon simulations. The dimensions of the coupon and the material properties are the same as in the $0^0/90^0$ coupon simulations. Figure 12 shows the front view of the coupon and a zoomed view of an extreme portion. The red color represents the in-plane shear failure of the coupon. The center portion of the coupon is failed in shear due to scissoring. Figure 13 compares the predicted average stress-strain response of ±45^0 coupon specimen (i.e. with and with-out inclusion of scissoring model in DyCrash) with that of the experiment. The black color curve shows the actual behavior observed in the experiments. It can be seen that the stress linearly increases with strain in the initial portion of the stress-strain curve. When the matrix fails, the tows behave compliantly and start to rotate in the direction of load, which is why the flat portion in the stress-strain curve occurs. As soon as the tows start jamming, the stress starts increasing linearly with strain which is evident in the third portion of the curve. The final failure is predicted to be due to the fiber failure. The gray and white colors represent the responses predicted with and without inclusion of the scissoring mechanism in the DyCrash module. The shear properties are calculated by tuning the average stress-strain response of ±45^0 coupons in the simulations and the experimentally observed behavior. It can be seen that the behavior predicted by including the scissoring mechanism matches the actual behavior, as observed in the experiments. The best estimates for the shear strength and non-linear parameter turn out to be 40MPa and 5.5, respectively.

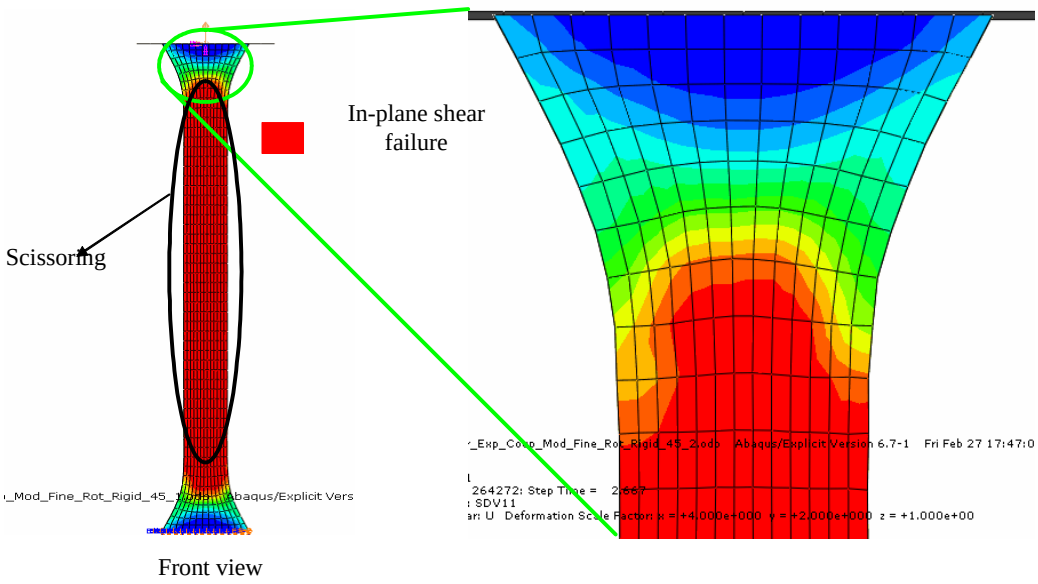

Figure 12: Shear failure of ±45^0 coupon in tension

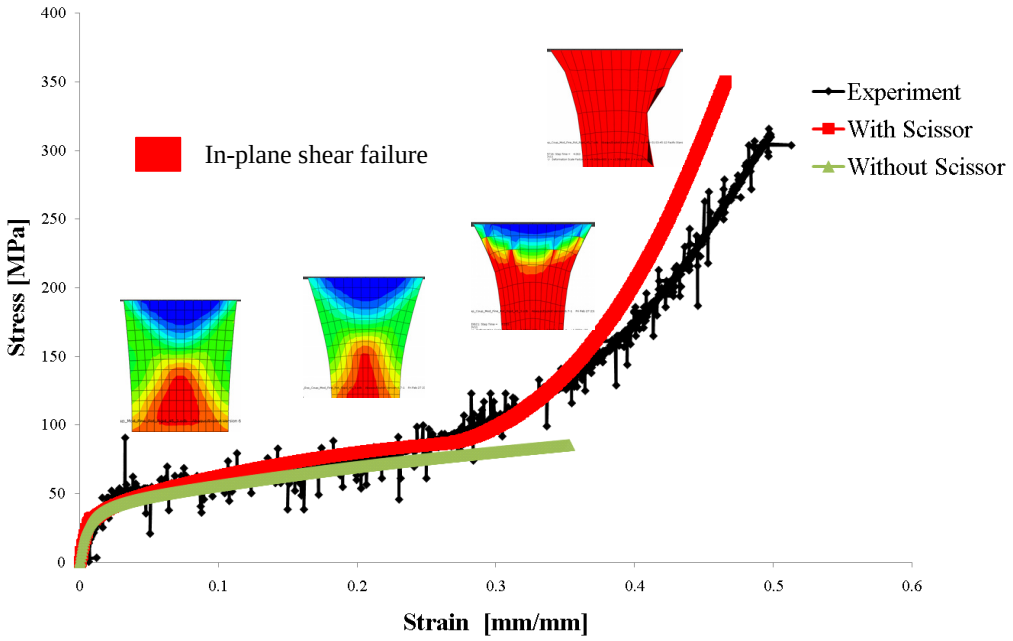

Figure 13: Comparison of average stress-strain response of Kevlar ±45^0 coupon

Conclusions

A DyCrash module is developed for LS-DYNA to simulate the crushing response of various textile composites. The DyCrash module needs unit-cell dimensions, tow, matrix properties, and visco-plastic parameters as its input. Each tow segment within the unit-cell is assumed to have elastic-viscoplastic behavior. An efficient homogenization scheme is employed to calculate the smeared properties of the unit-cell. A suitable model is implemented to account for stiffening

and scissoring phenomena, as observed in the coupon level tests. Currently, the DyCrash module is being validated for the Kevlar fabrics. Once fully validated, the DyCrash module can be used to optimize the energy absorption by selecting various fiber/matrix combinations with different textile architectures. The DyCrash can potentially be also used to simulate the ballistic behavior of Kevlar fabrics composites.

Acknowledgements

The authors would like to acknowledge the financial support of NASA under grant number NNX07AD04A.

References

1 Thornton P. H., "Energy absorption in composite structures," Journal of Composite Materials, 13, 247-262, 1979
2 Jackson K. E., "Impact testing and simulation of a crashworthy composite fuselage concept," International Journal of Crashworthiness 6 (1): 107-121 2001
3 Fasanella E. L. and Jackson K. E., "Impact testing and simulation of a crashworthy composite fuselage section with energy-absorbing seats and dummies," Journal of the American Helicopter Society 49 (2): 140-148 2004.
4 Ishikawa T. and Chou T. W., "Stiffness and Strength Behavior of Woven Fabric Composites," Journal of Materials Science, 17 (11): 3211-3220, 1982.
5 Naik R. A., "Failure Analysis of Woven and Braided Fabric Reinforced Composites," Journal of Composite Materials, 29 (17): 2334-2363, 1995.
6 Cox B. N., and Flanagan G., "Handbook of Analytical Methods for Textile Composites," NASA Contractor Report No: 4750, 1997.
7 Naik N. K. and Ganesh V. K., "An Analytical Method for Plain Weave Fabric Composites," Composites, 26: 281-289, 1995.
8 Tabiei A., and Ivanov I., "Materially and Geometrically Non-Linear Woven Composite Micro-Mechanical Model With Failure for Finite Element Simulations," Int. J. Non-Linear Mech., 39: 175–188, 2004.
9 Blackketter D. M., Walrath D. E., and Hansen A. C., "Modeling Damage in Modeling Damage in a Plain Weave Fabric-Reinforced Composite Material," Journal of Composites Technology and Research, 15(2): 136-142, 1993.
10 Beard S. J., Chang F-K., "Energy absorption of braided composite tubes," International Journal of Crashworthiness, 7 (2): 191-206, 2002.
11 Flesher N. D., "Crash Energy Absorption of Braided Composite Tubes," Thesis (Ph.D.)--Stanford University, 2006.
12 Janapala N. R., Chang F-K., "Crashworthiness of Rotorcraft Sandwich Structures Made of Kevlar Fabrics," NASA Contract No: NNX07AD04A, Year-2 report, 2009.
13 Yoon K. J. and Sun C. T., "Characterization of Elastic-Viscoplastic Properties of an AS4/PEEK Thermoplastic Composite," Journal of Composite Materials, 25: 1277-1313, 1991.
14 Weeks C. A., and Sun C. T., "Modeling Nonlinear Rate-Dependent Behavior in Fiber-reinforced Composites," Composites Science and Technology, 58 (3): 603-611, 1998.
15 Hill R., "The Mathematical Theory of Plasticity," Oxford, 1950.
16 Polanco M., Kellas S., and Jackson K. E., "Evaluation of Material Models within LS-DYNA® for a Kevlar/Epoxy Composite Honeycomb," AHS International 65th Forum and Technology Display, Grapevine, TX, 2009.